A Vibration Cavitation Sensitivity Parameter Based On Spectral and Statistical Methods

Authors: Kristoffer K. McKee[a*], Gareth L. Forbes[a], Ilyas Mazhar[a], Rodney Entwistle[a], Melinda Hodkiewicz[b], and Ian Howard[a]

[a] Department of Mechanical Engineering, Curtin University, GPO Box U1987, Perth, WA 6845 Australia *and* CRC for Infrastructure and Engineering Asset Management GPO Box 2434, Brisbane QLD 4001 Australia

[b] School of Mechanical and Chemical Engineering, The University of Western Australia, 35 Stirling Highway, Crawley, WA, 6009 Perth, Australia

* Corresponding Author. Tel: +61-8-9266-7892; Email address: k.mckee@curtin.edu.au

Abstract

Cavitation is one of the main problems reducing the longevity of centrifugal pumps in industry today. If the pump operation is unable to maintain operating conditions around the best efficiency point, it can be subject to conditions that may lead to vaporisation or flashing in the pipes upstream of the pump. The implosion of these vapour bubbles in the impeller or volute causes damaging effects to the pump. A new method of vibration cavitation detection is proposed in this paper, based on adaptive octave band analysis, principal component analysis and statistical metrics. Full scale industrial pump efficiency testing data was used to determine the initial cavitation parameters for the analysis. The method was then tested using vibration measured from a number of industry pumps used in the water industry. Results were compared to knowledge known about the state of the pump, and the classification of the pump according to ISO 10816.

Keywords: Condition Based Monitoring; Vibration; Cavitation; Centrifugal Pumps; Octave Band Analysis; Principal Component Analysis.

1. Introduction

There are 13 well defined fault modes of a pump, some of which are detectable using vibration monitoring. Cavitation is found to be one of the most common fault modes appearing in centrifugal pumps in industry due to the inability of the end user to constantly maintain the minimum needed pressure in the pipelines upstream of the pump. Usually undetectable upon inception, its presence during normal operation of the pump are usually not noticed until its effects have done considerable damage to the pump, (K. K. McKee, G. Forbes, I. Mazhar, R. Entwistle, & I. Howard, 2011).

This paper presents a method utilising adaptive octave band analysis techniques, where the octave bands are centred on the pump running speed, and statistical methods to determine the presence of cavitation using the measured centrifugal pump vibration velocity. A review of the state of the art in cavitation detection is presented in section 3. Section 4 then explains the theory behind the proposed method. The final sections of the paper then briefly describes the methodology and procedure used, and the results of case studies where the method has been applied to vibration data measured from industrial centrifugal pumps.

2. Cavitation

Cavitation is the formation of vapour bubbles in a moving fluid and their subsequent implosion within the centrifugal pump. The effects of this fault mode may have devastating impacts on the centrifugal pump, such as extreme local heating, high local pressures, energy being released, and extensive pitting on the impeller which would render the impeller inoperable, (Cudina, 2003; Yedidiah, 1996). Cavitation damage, which occurs on the low pressure or the visible surface of the impeller inlet vane, is accompanied by four symptoms: erosion via pitting of the impeller, a sharp crackling noise which is sometimes compared to pumping stones, high amplitude vibration, and a reduction in pumping efficiency, (K. K. McKee, et al., 2011; Palgrave, 1989; Rayner, 1995).

Pump designers attempt to avoid cavitation by taking into account the high and low capacities of the system when designing pumps, resulting in pumps that are most comfortable operating in the range of 90% to 110% of their best efficiency point (BEP) . However, problems arise since the majority of centrifugal pumps are forced to operate outside of this region, (Forsthoffer, 2011).

3. State of the Art in Cavitation Detection

Detection of the onset of cavitation is a difficult task to achieve. A large number of methods have been investigated to be able to predict and diagnose cavitation within pumps during operation. Despite the promising results from a number of reference works, no single method has been shown to be able to be deployed in all field situations.

M. Cudina utilized microphones to detect the onset of cavitation. Placing the microphones near the centrifugal pump, it was determined that a discrete frequency tone of half the blade pass frequency was distinct from the noise associated with the pump and thus was a clear indication of the onset of cavitation and its development. In later studies, Cudina et al determined that this distinct frequency was a function of the pump's design, such as the pump's geometry and material used, (Černetič & Čudina, 2011; Cudina, 2003; Čudina & Prezelj, 2009). The problems with this analysis are (1) it would be difficult for a technician to implement the detection method without knowing intricate information about the pump, and (2) surrounding noise from the environment could cause background noise interference in the signal, thus resulting in difficulty and possible inability of finding the distinct frequency

stated by Cudina. The use of vibration analysis to determine faults have been proven to be a more reliable method of fault detection over audible measurements.

Neil et al and Alfayez et al performed industrial scale tests to determine if acoustic emission sensors are able to detect cavitation. Both cases were found to show the onset of cavitation, while only one was able to show its existence. As a result, if acoustic emission sensors were to be used on a centrifugal pump, they would have to be attached on the pump from the factory and then observed frequently. They cannot be placed onto a used pump that has an unknown condition since the sensors are only able to reliably show the onset, and not the development of cavitation. In addition, although empirical evidence supports the validity of using acoustic emission sensors to detect incipient cavitation, limited evidence of the effectiveness of this technique for a wide range of industrial environments is found, (Alfayez, Mba, & Dyson, 2005; Neil, Reuben, Sandford, Brown, & Steel, 1997). This is opposed the proposed vibration analysis for cavitation, which can be used to detect cavitation in all its stages, from inception to complete development.

Cavitation models attempt to incorporate all factors involved in an effort to predict the behaviour of the cavitating state. However, despite their high accuracy, models have difficulties modelling the nonlinearities of cavitation as well as being insensitive to the operating point, (Athavale, Li, Jiang, & Singhal, 2002; Hofmann, 2001; Kallesoe, Cocquempot, & Izadi-Zamanabadi, 2006; Kallesoe, Izaili-Zamanabadi, Rasmussen, & Cocquempot, 2004; Uchiyama, 1998). As a result, a number parameters needed to accurately tune the model are difficult to obtain, and thus need to be assumed when not readily available. This leads to the development of inaccurate models. The proposed method for detecting cavitation removes the need to determine these modelling parameters and relies solely on the accepted levels of vibration velocities, which can be obtained using robust industrial accelerometers.

Some methods of cavitation detection utilise data other than vibration in their analysis. Methods such as measuring inlet pressure fluctuations are a good indicator of cavitation and have been shown to be more sensitive than comparing the actual net positive suction head (NPSHa) to the required net positive suction head (NPSHr). However, it is sometimes difficult to obtain this data due to the alterations that must be done to the pump to secure the instrumentation, (Franz, Acosta, Brennen, & Caughey, 1990; Jensen & Dayton, 2000; Lee, Jung, Kim, & Kang, 2002; Rapposelli, 2002). Other forms of analysis are able to use methods of non-destructive testing, such as the use of accelerometers, which attach to the outside of the pump without the need to alter it in any way to detect vibration. This saves time in the implementation phase of the method.

Parrondo et al created an expert system that attempted to detect the existence of six abnormal situations including flow rate greater than the best efficiency flow rate, lower flow rate, cavitation partially developed, cavitation fully developed, presence of an obstacle in the inlet conduit and rotational speed greater than or lower than the specified value. Although its classification of the pump's fault mode was correct on the lab tested setup, the effectiveness of adapting such a system to other industrial pumps was not attempted, (Parrondo, Velarde, &

Santolaria, 1998). Similarly, Yang et al (Yang, Lim, & Tan, 2005) created an expert system for fault detection for centrifugal pumps which also incorporated decision trees. The problem with expert systems is that they are normally system specific. In this case, 6 abnormal situations were attempted on a single system. However, parameters change based on factors such as the environment, size of pump, size of motor, and load; and thus, more investigation is needed to create a more versatile expert system. The proposed method for detecting cavitation is not limited by factors in the environment, and has been shown using experimental data to work on a variety of centrifugal pumps in different environmental conditions. As a result, it has been demonstrated to be more versatile and robust than Parrondo et al's expert system.

Sakthivel et al and Azadeh et al created a fuzzy logic system to identify up to 19 failure modes of a centrifugal pump. Classification was based on statistical features of a vibration signal, such as mean, standard deviation and kurtosis, as well as a few other measurable quantities, such as flow rate, discharge pressure and temperature. Empirical evidence shows moderate results of classification of the multiple faults, (Azadeh, Ebrahimipour, & Bavar, 2010; Sakthivel, Sugumaran, & Nair, 2010). The difficulty associated with using fuzzy logic systems is the complexity in the creation of the fuzzy rules, which are usually done by hand, and their limits. Despite this problem, the papers only provide verification for their work based on one pump each. The method proposed has been tested on a number of different centrifugal pumps, which shows its robustness in industrial applications.

Sakthivel et al further created a vibration based fault diagnostic system using a decision tree for a monoblock centrifugal pump. It utilised 9 different statistical features from the data, such as standard error, standard deviation, and kurtosis, to separate the data and detect if one of 5 different fault conditions were present in the pump. The faults that were simulated and tested for are bearing fault, seal fault, impeller fault, bearing and impeller fault together, and cavitation. The C4.5 decision tree algorithm was used to create the decision tree for classification, and resulted in a 100% accuracy for the training data and 99.66% accuracy for the testing data (Sakthivel, Sugumaran, & Babudevasenapati, 2010). Sakthivel et al had only tested their method on a single pump, and surmise that the same method can possibly be used in general on all pumps. One of the largest problems with using decision trees is training the system. Care must be given so as to not overtrain or under-fit the data. Overtraining will result in good results, such as that given, for the training data, and possibly from the testing data if they all come from the same source. However, taking the newly over-trained decision tree and presenting it with data from an unseen pump may result in poor results. Under-fitting will produce similar results for the test case, but can also produce poor results for the training case as well. The method proposed has been tested over a range of different sized pumps in a range of different conditions to show its robustness.

Reasonable accuracy in cavitation detection was obtained by Wang et al who utilised wavelet analysis, rough sets, and partially linearized neural networks (PNN). The system was able to correctly detect cavitation with an 85.1% accuracy, (H. Wang, 2010; Huaqing Wang & Chen, 2007, 2009). Overall, the use of neural networks to detect cavitation has resulted in

mixed results. Most research results have not been validated against measurements taken in industry, but instead use data created in a lab under ideal conditions or created under simulations, (Klema, Flek, Kout, & Novakova, 2005; Y. Wang, Liu Hou, Yuan Shou, Tan Ming, & Wang, 2009; Zouari, Sieg-Zieba, & Sidahmed, 2004). As a result, their ability to perform on industrial equipment has not been verified. The problem with using neural networks to detect cavitation is the complexity and time needed in training the classifier. A large range of sample data, along with their known condition, is needed in order to correctly train the neural network to detect cavitation on a wide variety of machines and environments, regardless of the type of input used. This is not always available. The proposed method provides a simpler, robust way of taking less data than that needed for the neural network, to determine the level of cavitation. As a result, it saves on time needed to implement by not needing training time, as in the case of a neural network, but rather depends on statistical means to determine the level of cavitation.

A further in depth review of the state of the art of detecting cavitation has been done by Sloteman (Sloteman, 2007) and Ashokkumar (Ashokkumar, 2011) which covers a variety of methods.

In summary, the method proposed in this paper:

- Utilizes no invasive methods to obtain the needed data to assess the centrifugal pump's health. Rather, it utilizes accelerometers, which can be placed on the top and side of the bearing housing for the centrifugal pump and attached using an adhesive, such as bees wax, or magnets. Hence, the implementation of the method in the field can easily be done by technicians.

- Does not rely on modelling parameters; nor does it rely on any method in which over-training or under-training can present a problem.

- Utilises principal component analysis and Mahalanobis distance, which have been found in the literature to be used separately to aid in cavitation detection but not together, in conjunction with an adaptive version of octave band analysis.

- The combination of the three techniques (principal component analysis, Mahalanobis distance, and adaptive octave band analysis) allows the data to be visualized in a normally distributed space.

- Takes advantage of the inherent normal distribution of the centrifugal pump's fault data through the use of Mahalanobis distance as a distance metric, to set thresholds on classifying data. These thresholds produce ellipsoids that define the boundaries between regions. Most thresholds are created based on a 2 class system, healthy and not-healthy, since the method utilized can either successfully detect incipient cavitation or fully formed cavitation well. This was the scene in Cudina et al's work (Cudina, 2003). As a result, most

researchers focus on a healthy pump versus a pump with fully formed cavitation.

- Classifies the health of the pump not only in 3 regions (healthy / no cavitation, incipient cavitation, fully formed cavitation), but it also provides the user with values to describe the severity within that level. This again is based on the Mahalanobis distance from the centre of the data.

- Has been tested on a wide range of types and sizes of centrifugal pumps to show its robustness to be used in any industrial setting.

4. Theory

4.1 Principal Component Analysis

Principal Component Analysis (PCA) is a method that maximizes the variance among variables. Input variables that are utilised are independent and without the assumption of clusters within the data. PCA produces a series of orthogonal principal components, which are a linear combination of the input variables, ordered according to the amount of spread of their variances, (Kim & Rattakorn, 2011; Rencher & Christensen, 2012). PCA is often used as a pre-processing technique to other methods such as clustering and artificial neural networks, (Cui, Li, & Wang, 2008; Jolliffe, 2005).

The goals of PCA are to (Abdi & Williams, 2010; Wold, Esbensen, & Geladi, 1987):

1. extract the most important information from the input data
2. compress the data set by removing non-important information
3. reducing / simplifying the data set
4. determine the relationships between objects

PCA is performed on a multivariate data matrix, denoted by **X**, where the *I* rows are the "observations" and *J* columns are termed "variables", (Wold, et al., 1987). The components of the PCA are obtained from the singular variable decomposition (SVD) of **X**:

$$\mathbf{X} = \mathbf{P}\Delta\mathbf{Q}^{\mathbf{T}} \qquad (1)$$

where **P** is the matrix of left singular vectors of the size *I x L*, **Q** is the matrix of right singular vectors of the size *J x L*, and **Δ** is the diagonal matrix of singular values. Let **F** be the *I x L* matrix of factor scores, which can be obtained by:

$$\mathbf{F} = \mathbf{P}\Delta. \qquad (2)$$

Factor scores are another name for the principal components, and can be interpreted as the projections of the observations onto the principal components. **Q** can then be interpreted in two ways. First, it provides the coefficients of the linear combinations that are used to create the factor scores, known as the "loading matrix". It is also the projection matrix of **X**

onto the principal components. Since the product of **Q** and its transpose, $\mathbf{Q}^T$, is the identity matrix, the equation for **F** can be transformed to include **Q** via, (Abdi & Williams, 2010):

$$\mathbf{F} = \mathbf{P\Delta} = \mathbf{P\Delta Q}^T\mathbf{Q} = \mathbf{XQ} \quad (3)$$

A geometric interpretation of PCA is best understood if **X** represents two variables whose data produces a skewed ellipse. An example is shown in Figure 1, which represents a set of sample data of RMS velocity vibrations measured radially from a centrifugal pump. The two axes represent the RMS values from two different sections in the frequency domain, called octave bands. Octave bands are explained in detail in section 4.2.

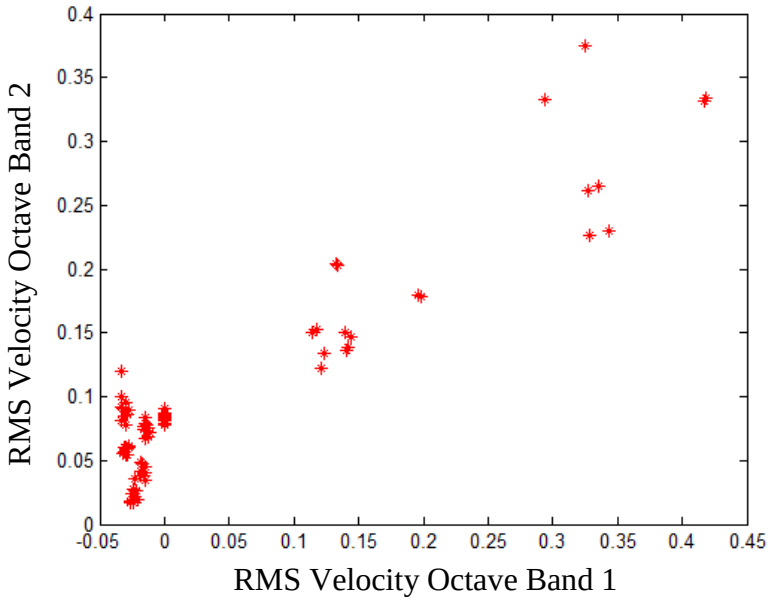

Figure 1: Sample Data of RMS Velocity Vibrations of a Centrifugal Pump

The first principal component provides the linear combination of both variables to produce the major axis of the skewed ellipse. This axis will contain the maximum variance, or spread, of the data. The second principal component provides the linear combination of both variables to produce the minor axis of the skewed ellipse. This orthogonal axis will contain the second largest variance of the data, (Abdi & Williams, 2010). The two principal axes for the data shown in Figure 1 are shown in Figure 2.

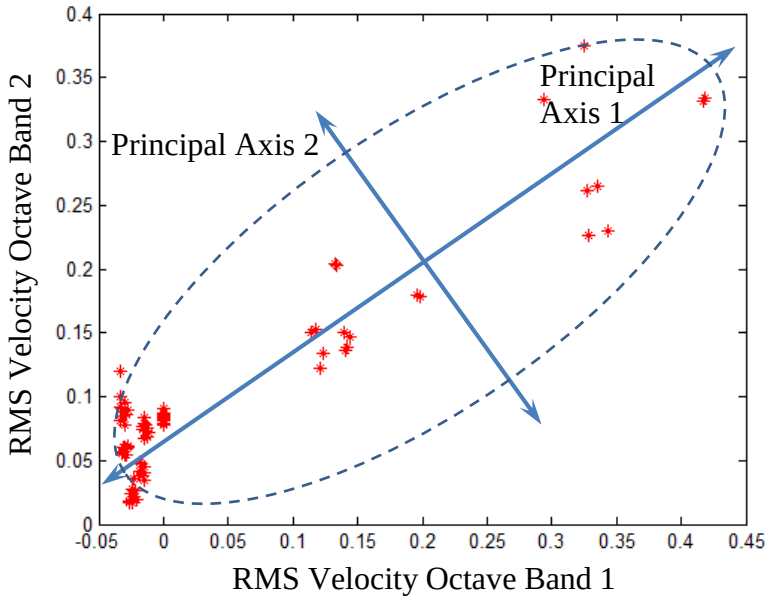

Figure 2: Sample Data With Principal Axes

Since PCA is a least squares method, outliers within the data greatly influence the model. As a result, it is imperative that outliers are corrected or eliminated prior to the PC model being created. Similarly, variables with little variance should be removed from the data set since they do not provide a lot of useful information, (Wold, et al., 1987).

4.2 Octave Bands

Octave bands have been used in the field of acoustics, where standards defined in documents such as ISO 532, divide the frequency spectrum into sections, or bands, centred on pre-defined central frequencies (cf), (Standardization, 1975). This division of the frequency spectrum into bands aids in determining where the energy in a signal is found, which may lead to determining the cause of the energy.

McKee et al have taken the concept of octave bands and adapted them to suit the need of rotating machinery vibration analysis, (K. K. McKee, Forbes, G., Mazhar, I., Entwistle, R. and Howard, I., 2012). To do so, the central frequency of the second octave band has been centred on the running speed (x) of the machine in Hertz. Subsequent octave bands have central frequencies that are double that of the previous ones (x, 2x, 4x, 8x, etc.) with lower limits and upper limits defined in the same way as that of ISO 532. The final octave band is defined as that which contains the upper limit of the sampling bandwidth. As a result, each octave band contains frequency information surrounding certain harmonics of the shaft speed of the machine. The first octave band contains sub-harmonic information about the machine, (K. K. McKee, Forbes, G., Mazhar, I., Entwistle, R. and Howard, I., 2012). A summary of the octave bands, their limits, and multiples of the running speeds found within them are found in Table 1.

Table 1: Limits and Running Speeds for adaptive Octave Bands

Octave Band	Lower Limit $\left(Y = \frac{x}{\sqrt{2}}\right)$	Upper Limit $(2Y = x\sqrt{2})$	Multiples of running speed (x) centre frequency
1	0	Y	Sub harmonic
2	Y	2Y	1x
3	2Y	4Y	2x
4	4Y	8Y	4x
5	8Y	16Y	8x
6	16Y	32Y	16x
7	32Y	64Y	32x
8	64Y	128Y	64x
9	128Y	256Y	128x
10	256Y	512Y	256x

An example of dividing the frequency spectrum into octave bands is found in Figure 3which shows the acceleration power spectrum measured radially on a bearing taken from a Thompsons, Kelly & Lewis centrifugal pump, 840 kW, operating at 741 rpm. By placing the octave band limits in Figure 3, the multiples of the running speed in Table 1, such as the running speed at 12.4 Hz and twice the running speed at 24.8 Hz, are shown as spikes at the centre frequencies of octave bands 2 and 3 respectively.

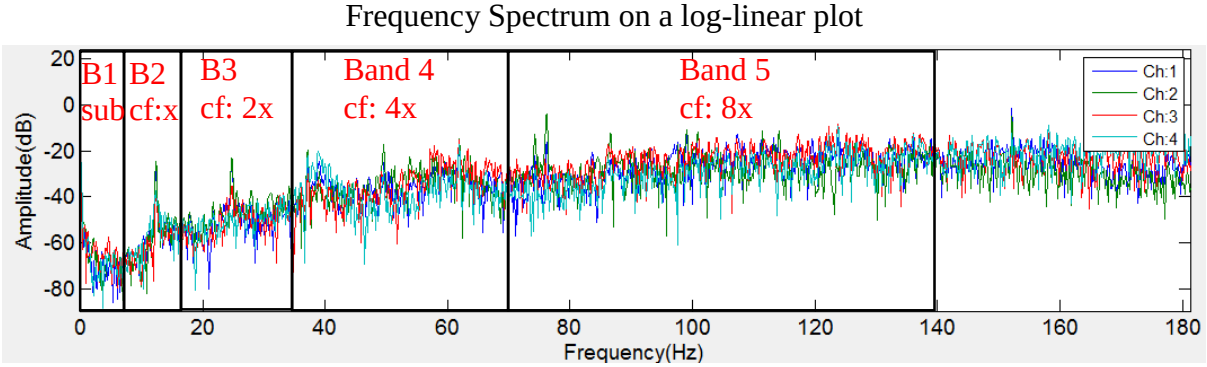

Figure 3: Octave Bands Centred On Running Speed (x = 12.4 Hz)

4.3 Mahalanobis Distance

Multivariate data analysis often requires distances between two points to be calculated. Two common distance measures are the Euclidean distance (ED) and the Mahalanobis distance (MD), both of which can be used in the original variable space and in the principal component space. Although ED is the easiest to apply and most common to use, MD provides insight into the data that helps better explain its distribution. MD is used in a variety of applications ranging from detection of outliers, selection of calibration samples

from measurements, choosing representatives of data sets, within clustering algorithms such as the k-Nearest Neighbour, as well as in discrimination techniques and class modelling techniques. MD is also found in the equation for multivariate normal distributions, (Cho, Hong, & Ha, 2010; De Maesschalck, Jouan-Rimbaud, & Massart, 2000). This is useful in the area of condition monitoring, which determines the health of a machine based on various methods and tools such as vibration, since it accommodates the non-linear relationships found within a machine. Random vibrations obtained from machines are commonly classified as normal distributions due to simplifying the acceleration or velocity signal with indicators such as the mean, the standard deviation, and the root mean square (RMS), (Toyota, Niho, & Peng, 2000).

Computation of MD is dependent on the ability to calculate the variance-covariance matrix. This computation causes problems when redundant or correlated information is found within the data set, as commonly found in data sets with large number of variables, and when the number of variables exceeds the number of objects in the data sets. Hence, MD is normally calculated after choosing a small number of significant original variables or principal components after performing PCA, (De Maesschalck, et al., 2000).

To compute the MD, the variance-covariance matrix $\mathbf{C_x}$ must be computed using the formula (P.-C. Wang, Su, Chen, & Chen, 2011):

$$C_x = \frac{1}{n-1}(X_c)^T(X_c) \quad \textbf{(5)}$$

where $\mathbf{X}$ is an n x p matrix containing n objects and p variables. $\mathbf{X_c}$ is a column-centred data matrix obtained by subtracting the mean of each column from every entry in the column. For the case of three variables, this equation simplifies to:

$$C_x = \begin{bmatrix} \sigma_1^2 & \rho_{12}\sigma_1\sigma_2 & \rho_{13}\sigma_1\sigma_3 \\ \rho_{12}\sigma_1\sigma_2 & \sigma_2^2 & \rho_{23}\sigma_2\sigma_3 \\ \rho_{13}\sigma_1\sigma_3 & \rho_{23}\sigma_2\sigma_3 & \sigma_3^2 \end{bmatrix} \quad \textbf{(6)}$$

where σ_1^2, σ_2^2 , and σ_3^2 are the variances of the first, second, and third variables, and $\rho_{12}\sigma_1\sigma_2$ is the covariance between variable 1 and 2, $\rho_{13}\sigma_1\sigma_3$ is the covariance between variable 1 and 3, and $\rho_{23}\sigma_2\sigma_3$ is the covariance between variable 2 and 3, (De Maesschalck, et al., 2000).

The MD for each object $\boldsymbol{x_i}$ from the mean $\bar{\boldsymbol{x}}$ is calculated by (De Maesschalck, et al., 2000; Fernández Pierna, Wahl, de Noord, & Massart, 2002; Zhang, Huang, Ji, & Xie, 2011):

$$MD_i = \sqrt{(x_i - \bar{x})C_x^{-1}(x_i - \bar{x})^T} \quad \textbf{(7)}$$

MD can be found in the multivariate form of the normal distribution, which is given by the equation:

$$f(x_i) = \frac{1}{|\Sigma|^{1/2}(2\pi)^{p/2}} e^{-\frac{1}{2}(x_i-\mu)\Sigma^{-1}(x_i-\mu)^T} \quad \textbf{(8)}$$

where **Σ** is the variance-covariance matrix of **X** and **μ** is the mean of the x_i. Visualized in two dimensions, $f(x_i)$ transforms the data into the shape of an ellipse, while in three dimensions it is seen as the shape of an ellipsoid. Points with equal densities can be determined by taking the natural logarithm of both sides, and rearranging to obtain the squared MD:

$$MD_i^2 = (x_i - \mu)\Sigma^{-1}(x_i - \mu)^T = 2\,ln\left(|\Sigma|^{1/2}(2\pi)^{p/2}f(x_i)\right) = constant \quad \textbf{(9)}$$

This is deemed an improved distance metric than the square of the Euclidean distance since for normally distributed data, the ED does not take into account the correlation of the data, (De Maesschalck, et al., 2000).

Comparing the multivariate form of the normal distribution with the univariate normal distribution, given by the equation:

$$f(x) = \frac{1}{\sigma\sqrt{2\pi}}e^{-\frac{1}{2}\left(\frac{x-\mu}{\sigma}\right)^2} \quad , \quad \textbf{(10)}$$

where σ is the standard deviation of the population, **Z** is then defined as the standard normal random variable and is given by the equation:

$$Z = \frac{x-\mu}{\sigma} = \sqrt{\left(\frac{x-\mu}{\sigma}\right)^2} \quad , \quad \textbf{(11)}$$

which resembles MD in the multivariate case:

$$MD_i = \sqrt{(x_i - \mu)\Sigma^{-1}(x_i - \mu)^T} \quad . \quad \textbf{(12)}$$

As a result, MD can be used as the standard normal random variable for the multivariate normal distribution and will be used as the distance metric in the proposed method, (De Maesschalck, et al., 2000).

5. Methodology

Vibration monitoring has been found to be a proven method of determining fault modes within centrifugal pumps. As a result, an increasing number of pump manufacturers have been equipping their pumps with on-board sensors to help the end-user diagnose the health of their pumps. These instruments, coupled with standards such as those published by the International Organization of Standards (ISO), enables the end user to determine the overall health of the pump. In particular for centrifugal pumps, ISO 10816 classifies the RMS velocity vibration of a centrifugal pump into one of four different zones. These four zones (A, B, C and D) categorise the machine as either being:

- A - newly commissioned
- B - acceptable for long term continuous use
- C - acceptable for short term but not long term use
- D - inoperable

Vibration limits for each zone are dependent on pump characteristics such as the power rating, location of the motor with respect to the pump, height of the motor shaft, and the pump's orientation. Although this method provides an overall indicator of the health of the pump, it does not provide insight into the detection of specific fault modes that are causing unhealthy vibrations, (Standardization, 1998, 2009).

Methods such as data driven models (statistical methods and artificial neural networks), knowledge based models (expert systems and fuzzy logic systems) and physical models can be used in addition to the RMS velocity vibration to determine the overall health of the machine. However, these methods require more information than is available to a technician that services the machine, as well as being costly in time and money to produce, (K. McKee, G. Forbes, I. Mazhar, R. Entwistle, & I. Howard, 2011). As a result, more efficient and cost effective methods are needed to diagnose the health of a pump.

McKee et al (K. K. McKee, Forbes, G., Mazhar, I., Entwistle, R., Hodkiewicz, M. and Howard, I., 2012) had adapted the octave band analysis to aid in discriminating between the causes of the deviations from a healthy to an unhealthy state. This broadband technique divides the frequency domain into octave bands, which are then characterised via their RMS values for either the acceleration or velocity signal. Since the number of octave bands obtained can be numerous, McKee et al proceeded to utilise PCA analysis to determine which octave bands would best be utilised to determine the existence of cavitation in the vibration signal. Three octave bands were chosen and a weighted sum of the RMS values of these octave bands were used to create an indicator sensitive to the onset and development of cavitation (CSP – cavitation sensitivity parameter). Based on their findings, octave bands 2, 8 and 9 were found to contain characteristics that best indicate if cavitation is present within the vibration signal. Octave band 2 contains vibrations from cavitation that occur at the running speed and octave bands 8 and 9 capture the high frequency components of the cavitation vibration. A problem associated with the CSP is the setting of the threshold value for the onset of cavitation, which according to the data presented, may vary from 0.2 to 0.8. As a result a CSP based on a weighted sum of the result of three octave bands may not be feasible, (K. K. McKee, Forbes, G., Mazhar, I., Entwistle, R., Hodkiewicz, M. and Howard, I., 2012).

The proposed method utilises the three adapted octave bands (2, 8, and 9) to determine the onset and existence of cavitation by different means. Octave band analysis has benefits over narrowband spectrum as it is able to compare pumps of different speeds, which is much more difficult for a narrowband technique. PCA will be used to transform the RMS velocity values from the three octave bands into principal components, which can then be plotted on a three dimensional scatter plot. Mahalanobis distance is then used as a metric to determine how far each point is from the centre of a cluster of vibration data from healthy centrifugal pumps. Based on empirical data, a threshold can be set to determine if incipient cavitation and full cavitation has occurred.

6. Experiment

6.1 Test Data

Data obtained for this section was taken under known ideal pump test conditions and were used to create threshold values for the proposed method. These threshold values were then tested against other pumps running in industrial settings which were known to have or not have cavitation occurring. Testing with data obtained from pumps in industrial settings provided validation under real world conditions, thus demonstrating its usefulness in the field.

Data was initially attained from pump tests on a Gould's 3700, 90 kW, 4 vane impeller, centrifugal pump which ran under a nominal speed of 2990 rpm. The experimental setup is found in Figure 4. Baseline data was obtained under close to ideal operating conditions for the centrifugal pump and then the pump was gradually caused to cavitate using a suction vacuum under a range of operating conditions on a purpose built test facility. Signals were recorded on 4 accelerometers and dynamic pressure transducers during this process. 5 sets of data were obtained, where each set contained entries showing the progression from a non-cavitating state to an emerging state of cavitation, and in some cases, a fully cavitating state. Each dataset consisted of the four accelerometer channels, (Blagrove, 2003):

- Channel 1 was located radially on the non-drive end bearing
- Channel 2 was located axially on the non-drive end bearing
- Channel 3 was located on the Suction flange
- Channel 4 was located on the discharge flanges

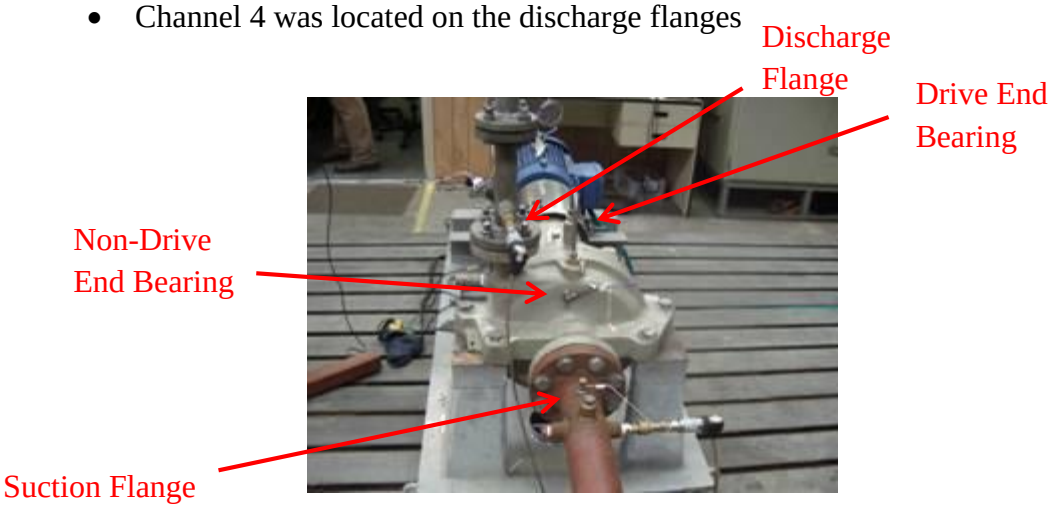

Figure 4: Gould's 3700 Pump Testing for Incipient Cavitation

Figure 5 shows four graphs, each a plot of the RMS Velocity Vibration values for each of the four channels in the dataset. Octave band 2, 8, and 9 were used to determine the RMS velocity levels, which have been plotted in a 3-D configuration as shown in Figure 5. Blue '*' points are data points declared as being vibrations from a "healthy pump", otherwise known as absent of a cavitation state. Green 'o' points are data points obtained during the cavitation incipient state. Incipient cavitation points were determined by Hodkiewicz while

collecting data by determining when the NPSHa was less than the NPSHr, (Hodkiewicz, 2012).

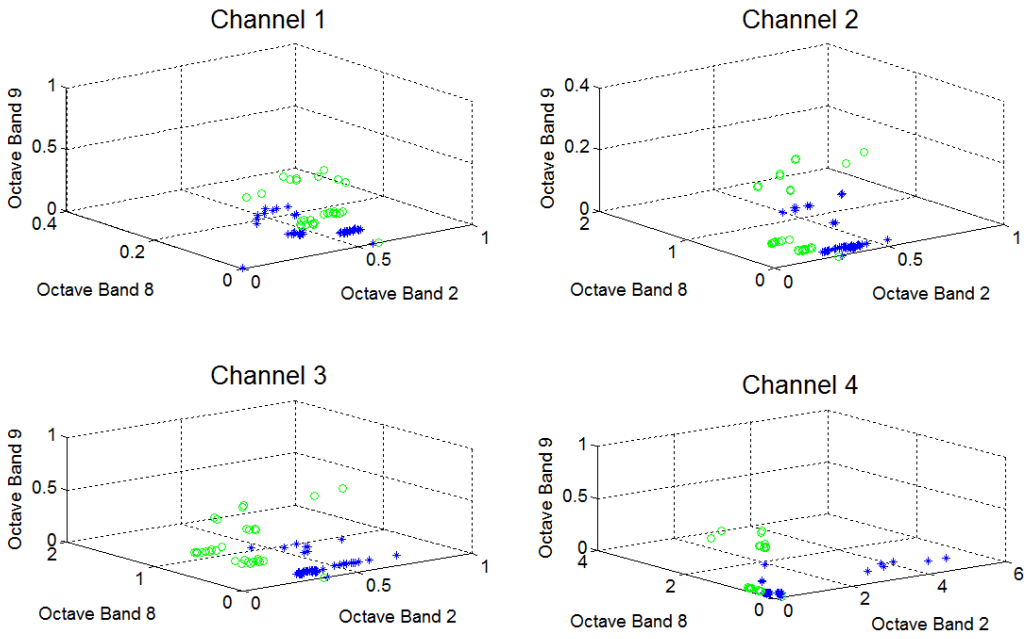

Figure 5: Non-Cavitating and Incipient Cavitating Data from Hodkiewicz's Data (Hodkiewicz, 2012)

The data viewed in Figure 5 shows signs of being separable between the non-cavitating and incipient cavitating data. As a result, a set of orthogonal axes was created that would maximize the separation of the two types of data for clustering purposes. PCA was performed on the three octave bands for each channel shown in Figure 5 to determine the optimal set of orthogonal axes that would be able to isolate both states from one another. The results of PCA are found in Figure 6. Figure 6 shows the same data found in Figure 5 plotted along a new set of orthogonal axes that best separate the two types of data, first along the first principal component axis, then along the second, and finally along the third after the axis has been rotated to provide a better view of the separated data.

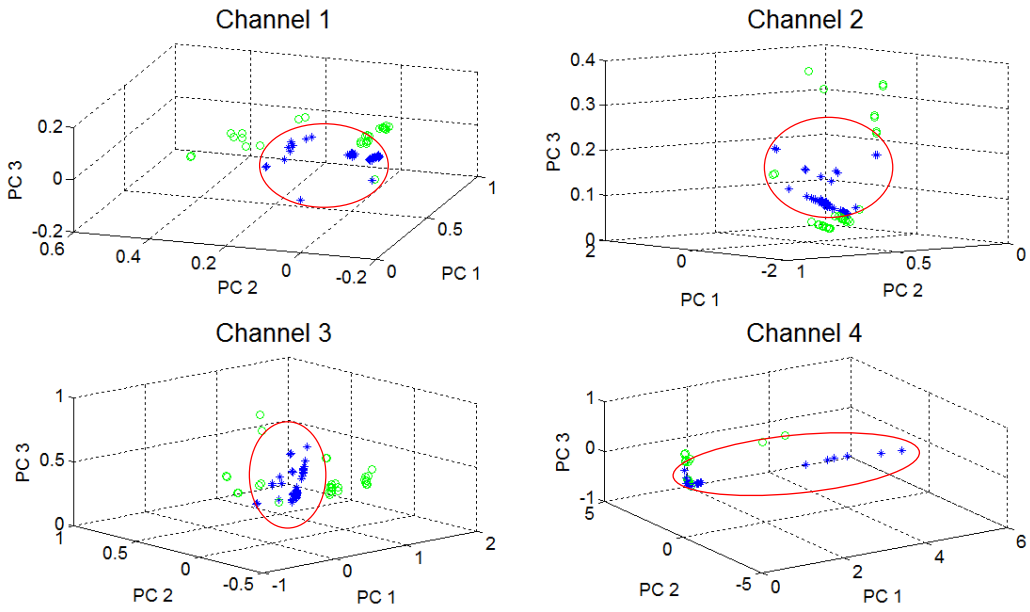

Figure 6: Rotated Axis of Plotted Principal Components

An ellipse has been placed around the non-cavitating data cluster in Figure 6 for all channels to show the possible separation of the two data clusters. The graphs show that the healthy data set can lie within a defined cluster, while most of the incipient cavitation data would lie outside of cluster, with minimal overlap. Although the data found in all four channels seemed promising to perform the next step in the analysis, only Channel 1 was chosen. This is due to the fact that most data for condition monitoring purposes are collected radially on the bearing. Axial bearing data is not always available, depending on which bearing was used for monitoring purposes. Suction and discharge flanges are not always used as locations of data collection since it is surmised that vibrations found at these locations would be felt in the bearings. In addition, Hodkiewicz et al had determined that the best location to monitor cavitation impacting on the pump impeller was at the horizontal position of the non-drive end bearing since it was indirectly mechanically coupled to the impeller. Axial bearing data had been shown to poorly reflect cavitation due to poor mechanical coupling with hydraulic excitation mechanisms. An accelerometer found on the suction flange was also found to be a suitable position, however the discharge flange was not found to be a suitable position for cavitation detection, (Blagrove, 2003). As a result, since the goal is to determine one position where a technician can perform data collection for cavitation, the Channel 1 accelerometer mounted radially on the bearing was utilised for further investigation in this study.

Assuming a normal distribution for the vibration data, an ellipsoid was placed onto the principal component axes of Channel 1. The variance-covariance matrix used to determine the shape and axes of the Gaussian multivariate normal distribution ellipsoid were calculated using only the healthy data. Moving incrementally by 0.05 standard deviations, it

was found that 1.85 standard deviations produced an ellipsoid that contained no incipient cavitating data and 20 out of 51 healthy points outside of the ellipsoid. This would produce a 39.2% misclassification error. This Gaussian ellipsoid is shown in Figure 7. Likewise, 4 standard deviations would include all non-cavitating data within the Gaussian ellipsoid and 22 out of 30 incipient cavitation points inside the ellipsoid as shown in Figure 8. This would produce a 73.3% misclassification error.

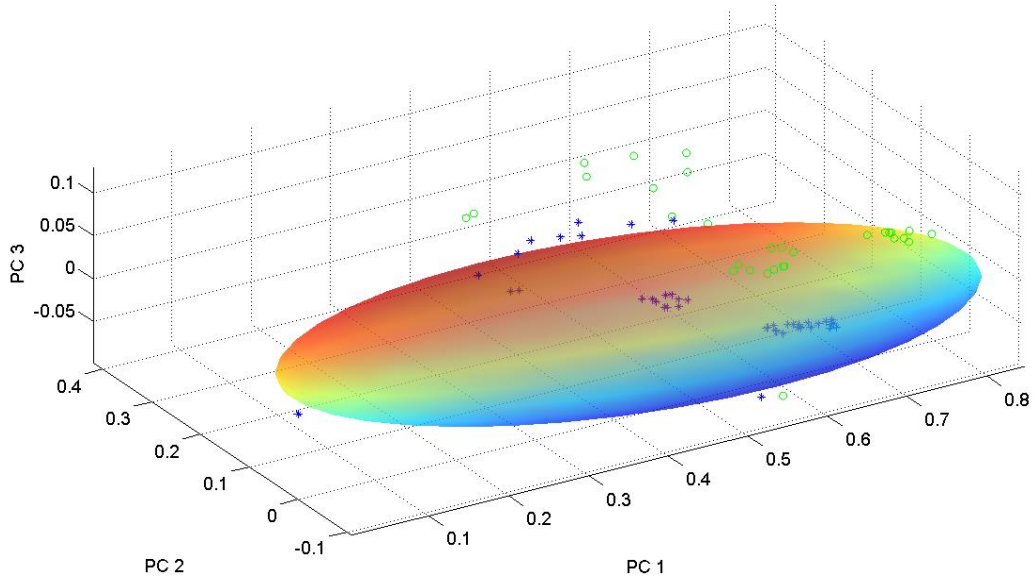

Figure 7: Gaussian Ellipsoid with 1.85 Standard Deviations

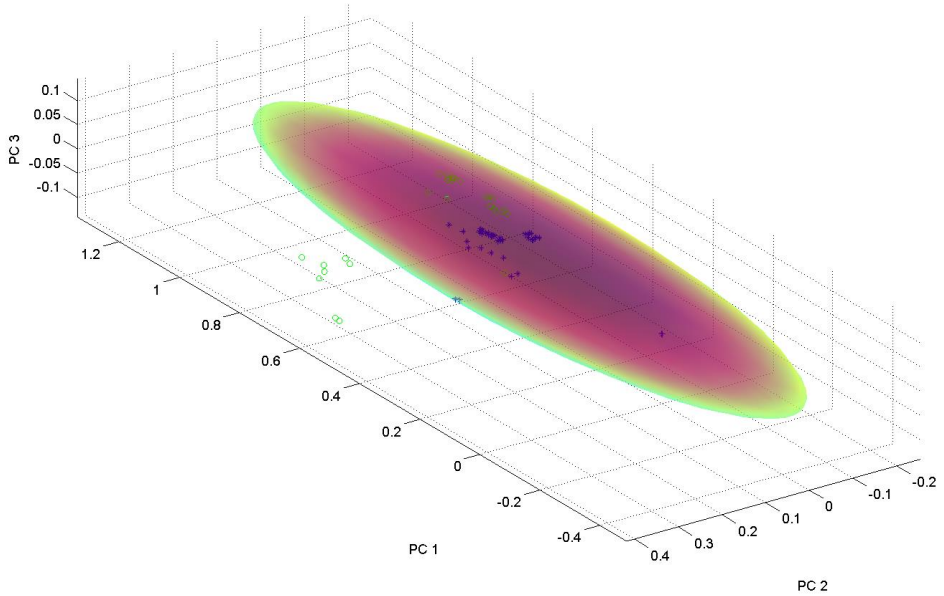

Figure 8: Gaussian Ellipsoid with 4 Standard Deviations

Table 2 shows the number of points correctly classified as the standard deviation changes from 3 to 1.85. Assuming a Gaussian multivariate normal distribution, points with a standard deviation of 3 or higher implies that the points are outliers to the healthy data, and thus are in the incipient cavitation state.

Table 2: Percentage of Correct Classification Based on Standard Deviation

Standard Deviation (σ)	**Normal Distribution (Percentage)**	**No Cavitation (Out of 51 Points)**	**No Cavitation (Percentage)**	**Incipient Cavitation (Out of 30 Points)**	**Incipient Cavitation (Percentage)**
3.0	*99.73*	*48*	*94.12*	*10*	*33.33*
2.9	99.62	48	94.12	11	36.67
2.8	99.48	48	94.12	11	36.67
2.7	99.30	48	94.12	12	40.00
2.6	99.06	48	94.12	18	60.00
2.5	98.76	48	94.12	20	66.67
2.4	98.36	48	94.12	22	73.33
2.3	97.86	48	94.12	23	76.67
2.2	97.22	48	94.12	24	80.00
2.1	*96.42*	*48*	*94.12*	*24*	*80.00*
2.0	95.45	42	82.35	25	83.33
1.96	*95.00*	*42*	*82.35*	*28*	*93.33*
1.9	94.26	32	62.75	29	96.67
1.85	*93.56*	*31*	*60.78*	*30*	*100.0*

Table 2 shows 4 values that are significant, which are standard deviations of 3, 2.1, 1.96 and 1.85. These values should be taken into account when determining the threshold values for cavitation. Figure 9 shows a schematic that helps explain the importance of these values.

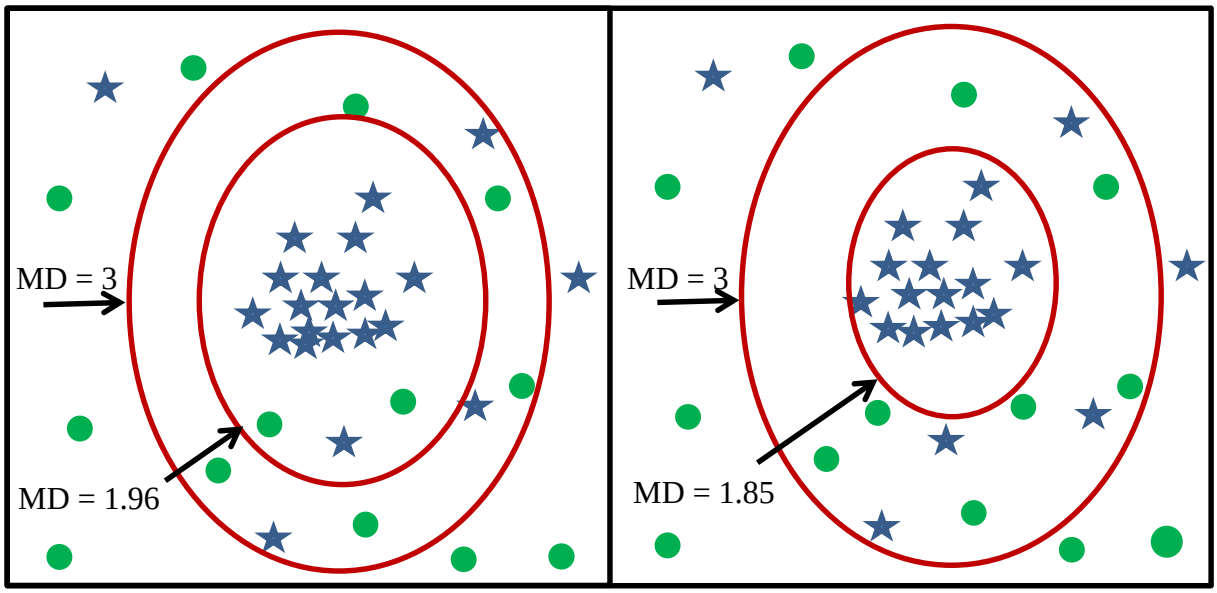

Figure 9: Schematic of Thresholds for Classification (not actual values)

(★ Non Cavitation, ● Incipient Cavitation)

A standard deviation of 1.85 was shown to correctly classify all the incipient cavitation points, as shown on the right side of Figure 9. A standard deviation of 1.96 should contain 95% of the healthy data, but instead correctly classifies 82.35% of the healthy data and 93.33% of the incipient cavitation data, as shown on the left side of Figure 9. This value minimizes the difference in percentage of points correctly classified in each of the categories. A standard deviation of 2.1 which represents 96.42% of the healthy data resembles closest to the actual spread of the healthy data, correctly classifying 94.12% of the healthy data and 80% of the incipient cavitation data. This value minimizes the difference in percentage of points correctly classified in each of the categories while minimizing the difference between the normal distribution percentage and the number of cavitation points correctly classified.

As a result of this analysis, a conservative set of thresholds and a more liberal set of thresholds can be devised to determine the existence of incipient cavitation. The conservative set of thresholds would ensure that all possible points of incipient cavitation are correctly classified, while the liberal set of thresholds would attempt to balance the amount of correctly classified points in each category. The value of 1.96 MD was chosen instead of 2.1 MD so as to err on the side of caution when classifying incipient cavitation. Hence, the data would be broken into three regions: No cavitation, Incipient Cavitation, Full Cavitation. Table 3 shows these thresholds. In addition, it is proposed that the severity level of the cavitation would be determined by the MD's data value, where the higher MD value would equate to a more severe state of cavitation.

Table 3: Thresholds for Cavitation

Thresholds	No Cavitation	Incipient Cavitation	Full Cavitation
Conservative	$0 \leq MD < 1.85$	$1.85 \leq MD < 3$	$MD > 3$
Liberal	$0 \leq MD < 1.96$	$1.96 \leq MD < 3$	$MD > 3$

6.2 Field Data

To test the thresholds and determine how well they are able to separate data from cavitating and non-cavitating pumps, accelerometer readings from four different industrial pump sets were obtained. Three sets contained pumps that were cavitating, while one set contained pumps that were not cavitating. Table 4 contains the manufacturer, type, power and running speed of each pump. The Thompsons, Kelly & Lewis pumps were employed by Sunwater, Queensland, Australia, to pump freshwater from lakes or reservoirs to neighbouring towns for household and commercial use. Two cavitating pumps were found at their Monduran site, pumping water out of Lake Monduran. Four pumps with no discernible signs of cavitation were found at their Bocoolima site, all of the same type, pumping water out of the Awoonga Dam. Even though the pumps at the Bocoolima site did not show signs of full cavitation, incipient cavitation may be occurring that did not provide warning signs that were visible to the end user.

The ITT Flygt pump was employed by Gold Coast Water, Queensland, Australia, to pump sewage waste water from neighbouring towns to nearby treatment plants. The two pumps at this site were known to cavitate often since the amount of incoming water varied throughout the day, thus not providing a constant amount of pressure on the suction side of the pump, (Sunwater, 2012).

Table 4: Pumps and Conditions

Pumps with No Discernible Cavitation (mixture of not cavitating and possible incipient cavitation)	Pumps with Full Cavitation
1. Thompsons, Kelly & Lewis 400x450 ECSD three stage pump, LSE 2600 kW, 1485 rpm	1. Thompsons, Kelly & Lewis 33”/36” SDS-DV, 840 kW, 741 rpm 2. Thompsons, Kelly & Lewis 24”/27” SDS-DV, 446 kW, 986 rpm 3. ITT Flygt CT-3231, 2 Blade, 85kW, 1475 rpm

All four data sets were plotted onto the two graphs, shown in 13. Non-cavitating data was plotted using blue ‘*’, cavitation inception data was plotted using green ‘o’, and fully developed cavitation data was plotted using red ‘+’. The left graph shows all points plotted with an inner ellipse of 1.85 MD and an outer ellipse of 3 MD, thus analysing the effectiveness of the conservative threshold values. The right graph shows all points plotted with an inner ellipse of 1.96 MD and an outer ellipse of 3 MD, thus analysing the

effectiveness of the liberal threshold values. In total, 197 data points were obtained from pumps that had cavitation and 93 data points were obtained from pumps that were reported as not cavitating. This last set of 93 data points may be representative of pumps that have incipient cavitation, which as described earlier, are currently undetectable using standard vibration analysis techniques for pump condition monitoring.

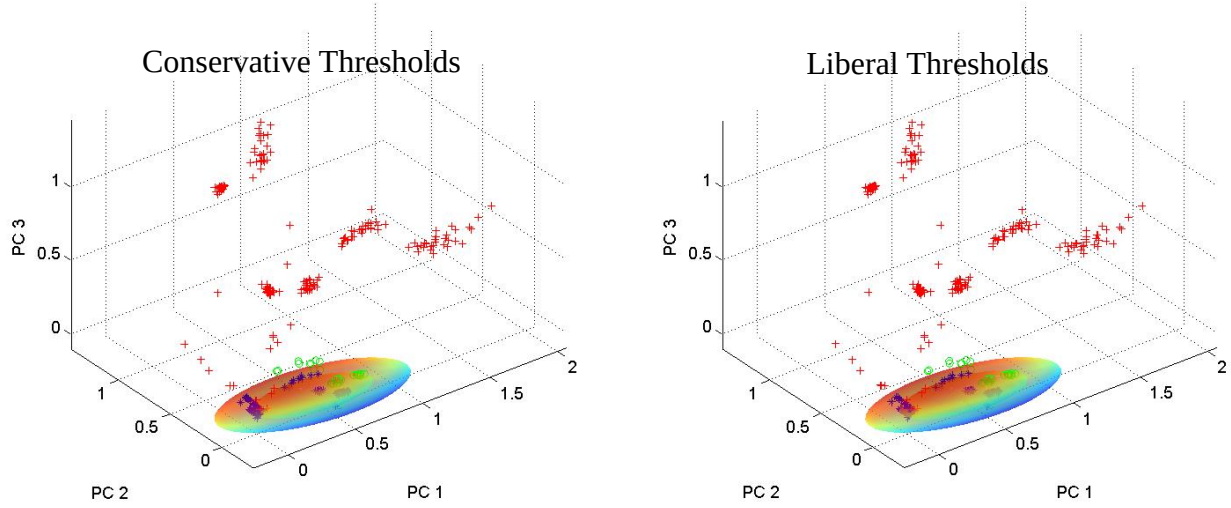

Figure 10: Industrial Pump Data with Conservative and Liberal Thresholds

(* Non-cavitating, o Cavitation inception, + Fully Developed Cavitation)

The results of the two plots in Figure 10 are divided into two tables. Table 5 shows 287 data points classified into one of three categories based on the two different types of thresholds. Table 6 shows the number of points known to be misclassified according to the thresholds, based on what is known about the pump. Points known to be operating with full cavitation but labelled as incipient cavitation, and points known to have no discernible cavitation but labelled as full cavitation were considered misclassified.

Table 5: Classification of Industrial Centrifugal Pump Data

	Non-Cavitating	**Incipient Cavitation**	**Full Cavitation**
Conservative	64	29	194
Liberal	76	17	194

Table 6: Misclassification of Industrial Centrifugal Pump Data

	Non-Cavitating	**Incipient Cavitation**	**Full Cavitation**
Conservative	1	2	0
Liberal	1	2	0

Table 5 shows that the two different limits on non-cavitating data caused 12 out of 93 points to be classified in a different category. This is shown as the difference between the number of points classified in the non-cavitating region (76 – 64), as well as the difference in the number of points classified in the incipient cavitation region (29 – 17). This results in a 13% difference in classification. However, none of these points were falsely classified as having full cavitation. Three out of the 197 points from the data known to have full cavitation had been classified as having incipient cavitation or non-cavitating, and are thus considered to be misclassified. Thus, a 1.5% misclassification of the data occurred. Table 7 shows the comparison of the classification results obtained in Table 5 compared to the classification given by ISO 10816.

Table 7: Data Points Classified by ISO 10816

	Non-Cavitating		**Incipient Cavitation**		**Full Cavitation**	
Conservative	*A*	63	*A*	28	*A*	92
	B	1	*B*	1	*B*	100
	C	0	*C*	0	*C*	9
	D	0	*D*	0	*D*	0
Liberal	*A*	75	*A*	16	*A*	92
	B	1	*B*	1	*B*	100
	C	0	*C*	0	*C*	9
	D	0	*D*	0	*D*	0

Table 7 shows that for the non-cavitating and incipient cavitating classifications, the results are in agreement with what is expected from ISO 10816. However, for those points known to come from a fully cavitating pump, in both cases, the results differ from what is expected from ISO 10816. ISO 10816 classifies 92 of these points as coming from newly commissioned pumps, 100 of these points as coming from a pump that is suitable for long usage, and only 9 of these points as coming from a pump that is usable only in short term and not long term.

As a result, it can first be concluded that cavitation can go undetected by using overall RMS velocity values, and thus undetected by ISO 10816. Since the contributions of cavitation to the overall vibrations are small amplitude increases in the high frequency regions as well as amplitude increases around the running speed of the pump, the amplitude increase of the overall RMS velocity values may not be large enough to signify the onset and initial stages of cavitation. Alterations to ISO 10816, such as implementing the use of octave bands and altering the limit for each octave band at each severity level of the ISO, as shown

in previous work (K. K. McKee, Forbes, G., Mazhar, I., Entwistle, R. and Howard, I., 2012), would allow for better detection of the fault modes. However, general limitations placed on these octave bands take into consideration the importance of increases in these frequency ranges, but do not take into consideration the behaviour of a specific fault mode as it appears in the vibration. As a result, it is necessary to create methods that set limits based on the behaviour of the fault mode to detect its existence in various frequency ranges.

Secondly, it has been shown that RMS velocity of high frequency vibrations and once per revolution vibrations, as found in octave bands 2, 8, and 9 are able to detect and classify the severity of the existence of cavitation within a centrifugal pump when thresholds are applied based on a multivariate normal distribution values. The difference between utilising adaptive octave bands in this research, as well as in (K. K. McKee, Forbes, G., Mazhar, I., Entwistle, R. and Howard, I., 2012), and the normal use of octave bands is that the second octave band is centred around the running speed of the pump. As a result, the upper and lower limits, and the centre frequencies of each octave band changes as the running speed of the pump changes. This causes the octave bands to consistently have the same multiples of the running speed in the same octave bands regardless of the actual running speed of the pump, rather than octave bands only containing values of the signal at the same frequencies each time. As a result, comparing and tracking changes in the behaviour of a machine becomes easier since statistical information would be dependent on behaviours that appear around multiples of the running speed of the pump. By applying a multivariate normal distribution ellipsoid based on the behaviour of non-cavitating data and incipient cavitation data, the statistical behaviour of RMS velocity vibration in the octave bands can be utilised to create limits that better represent the vibration behaviour of a cavitating pump.

Due to the simplicity and effectiveness of this method, it is recommended for employment into field use. To do so, the technician would first need to download the processed data and its covariance matrix that was used to create the thresholds for this method. From this point on, field technicians would then only have to acquire data from accelerometers placed radially on the bearings. This data can easily be post processed into octave bands, and the RMS velocity of octave bands 2, 8 and 9 can be obtained and measured from the centre of the ellipse obtained followed by using MD to produce a value representative of the cavitation state of the pump. This post processing of the data can be done on site in a matter of seconds on a velocity vibration signal of less than 1 minute duration. Hence, if placed onto a laptop or handheld device, this procedure can provide a technician with an instantaneous evaluation of the cavitation state of the pump.

7. Conclusion

This paper has presented an approach to perform cavitation detection based on octave band analysis, PCA, and statistical methods. Data sets from a 90 kW industrial pump without cavitation and a pump with incipient cavitation were used to create the variance-covariance matrix needed to obtain the parameters to treat the training dataset as a normal distribution.

MD was used as a distance metric to determine the severity of the cavitation and set threshold levels to divide the data sets into 3 states – non-cavitating, incipient cavitation, and full cavitation. Two types of thresholds were presented based on the trial training data to determine when incipient cavitation occurs. The method was then used on data obtained from 8 pumps of varying sizes and operating conditions used in the water industry to classify their operating condition compared to their known state. The presented analysis was able to identify all cavitation conditions within the 8 sets of field pump data only over specifying the cavitation level in 1.5% of cases. This analysis would have great advantage if combined in the implementation of an expert system, such as an expert fault tree diagnostic system, for industries utilising pump infrastructure.

7.1 Research limitations

Although the presented analysis was shown to be very robust with the given measurements, two limitations still exist which if overcome would allow even greater application of the method. Firstly due to the use of PCA, on a small number of data points, the removal of outlier data points was required. This needs to be done by a knowledgeable analyst with the application of their judgement. Obviously the need to remove outlier data points limits the automation of any method and removal of this criteria would enhance its application. This can somewhat be alleviated with the use of a larger number of datasets.

The next limitation which was not explored in this paper is if different fault modes would display similar characteristics in the fault indexes and therefore show up as pump cavitation when in fact it was another fault type present. This miss diagnosis of a fault type would need to be further investigated in future work.

7.2 Research contributions

This study extends the work of McKee et al (McKee, et al., 2012) and De Maesschalck et al. (De Maesschalck, et al., 2000) in using a reduced set of vibration characteristic measurements by applying PCA to spectral Octave band vibration measurements. The use of MD as a distance metric provides a more appropriate measure of the three dimensional PCA axes the data is projected onto. The results show only a 1.5% misclassification rate for the field data, suggesting that the above method is widely applicable and robust given the wide range of machine size and power ratings that was used for the research. It is believed that the displayed robustness in application is the strongest aspect of the presented work. Firstly, the robustness of this method comes from the use of the PCA selected Octave spectral based measurements. The selected bands, being: running speed and 8x and 9x running speed reinforce the knowledge that cavitation type faults contain spectral information at high frequencies and around the running speed. The subtle yet powerful method of setting the Octave band centre frequency based on the running speed is the next major contributor to the robustness of the presented analysis. The adaptive Octave band selection based on running speed allows for the generalisation of the method across different size pumps and operating conditions. These two initiatives in the analysis procedure culminate in a process for determining cavitation type faults without the need to calibrate for pump size or running

speed, nor requires detailed knowledge of specific pump details (which are often not readily available to technicians).

7.3 Research future directions

The most needed future expansion of the work presented within this paper is to apply the method to a larger variety of pumps running at different operating conditions and known fault levels to further gain insight into how widely it can be applied and to continue to test its robustness.

In terms of extending the theory of this method in future work, the integration of further pump performance data, such as motor current, flow rate and pressure level, along with vibration based measurements into the principal fault indicators would no doubt aid in the wider application of the procedure. It is believed that inclusion of additional pump performance data would help alleviate the ambiguity that can arise where other fault types may display similar vibration characteristics as cavitation.

Finally, this vibration based pump cavitation diagnostic analysis needs to be integrated into a wider fault diagnosis expert system to realise its full potential. This would particularly require further work for instance in automating the weighting given to the vibration based fault characteristics as compared to perhaps the pump performance based indicators to give an overall cavitation fault detection level.

8. Acknowledgements

This research was conducted within the CRC for Infrastructure and Engineering Asset Management, established and supported under the Australian Government's Cooperative Research Centres Programme. The authors would like to thank Gold Coast Water and Sunwater for facilitating the vibration measurements on the industrial water pumps used for the validation measurements.

9. References

Abdi, H., & Williams, L. J. (2010). Principal component analysis. *Wiley Interdisciplinary Reviews: Computational Statistics, 2*, 433-459.

Alfayez, L., Mba, D., & Dyson, G. (2005). The application of acoustic emission for detecting incipient cavitation and the best efficiency point of a 60kW centrifugal pump: case study. *NDT & E International, 38*, 354-358.

Ashokkumar, M. (2011). The characterization of acoustic cavitation bubbles – An overview. *Ultrasonics Sonochemistry, 18*, 864-872.

Athavale, M. M., Li, H. Y., Jiang, Y., & Singhal, A. K. (2002). Application of the Full Cavitation Model to Pumps and Inducers. *International Journal of Rotating Machinery, 8*, 45 - 56.

Azadeh, A., Ebrahimipour, V., & Bavar, P. (2010). A fuzzy inference system for pump failure diagnosis to improve maintenance process: The case of a petrochemical industry. *Expert systems with applications, 37*, 627-639.

Blagrove, L. (2003). *Cavitation Detectiion in Centrifugal Pumps using Vibration Signals and Fractal Analysis.* University of Western Australia Perth.

Černetič, J., & Čudina, M. (2011). Estimating uncertainty of measurements for cavitation detection in a centrifugal pump. *Measurement, 44*, 1293-1299.

Cho, S., Hong, H., & Ha, B.-C. (2010). A hybrid approach based on the combination of variable selection using decision trees and case-based reasoning using the Mahalanobis distance: For bankruptcy prediction. *Expert systems with applications, 37*, 3482-3488.

Cudina, M. (2003). Detection of Cavitation Phenomenon In A Centrifugal Pump Using Audible Sound. *Mechanical Systems and Signal Processing, 17*, 1335-1347.

Čudina, M., & Prezelj, J. (2009). Detection of cavitation in operation of kinetic pumps. Use of discrete frequency tone in audible spectra. *Applied Acoustics, 70*, 540-546.

Cui, P., Li, J., & Wang, G. (2008). Improved kernel principal component analysis for fault detection. *Expert systems with applications, 34*, 1210-1219.

De Maesschalck, R., Jouan-Rimbaud, D., & Massart, D. L. (2000). The Mahalanobis distance. *Chemometrics and Intelligent Laboratory Systems, 50*, 1-18.

Fernández Pierna, J. A., Wahl, F., de Noord, O. E., & Massart, D. L. (2002). Methods for outlier detection in prediction. *Chemometrics and Intelligent Laboratory Systems, 63*, 27-39.

Forsthoffer, W. E. (2011). 2 - Pump Best Practices. In *Forsthoffer's Best Practice Handbook for Rotating Machinery* (pp. 25-91). Boston: Butterworth-Heinemann.

Franz, R., Acosta, A. J., Brennen, C. E., & Caughey, T. K. (1990). The Rotordynamic Forces on a Centrifugal Pump Impeller in the Presence of Cavitation. *Transactions of ASME: Journal of Fluids Engineering, 112*, 264 - 271.

Hodkiewicz, M. (2012). Personal Conversation on Cavitation Data. In. Perth.

Hofmann, M. a. S., B. and Coutier-Delgosha, O. and Fortes-Patella, R. and Reboud, J.L. (2001). Experimental and Numerical Studies on a Centrifugal Pump with 2D-Curved Blades in Cavitating Condition. In *CAV 2001: Fourth International Symposium on Cavitation*. California Institute of Technology, Pasadena, CA USA.

Jensen, J., & Dayton, K. (2000). Detecting Cavitation in Centrifugal Pumps. In *Orbit* (Vol. 2, pp. 26 - 30). Nevada: GE Energy.

Jolliffe, I. (2005). Principal Component Analysis. In *Encyclopedia of Statistics in Behavioral Science*: John Wiley & Sons, Ltd.

Kallesoe, C. S., Cocquempot, V., & Izadi-Zamanabadi, R. (2006). Model based fault detection in a centrifugal pump application. *Control Systems Technology, IEEE Transactions on, 14*, 204-215.

Kallesoe, C. S., Izaili-Zamanabadi, R., Rasmussen, H., & Cocquempot, V. (2004). Model based fault diagnosis in a centrifugal pump application using structural analysis. In *Proceedings of the 2004 IEEE International Conference on Control Applications.* (Vol. 2, pp. 1229-1235 Vol.1222).

Kim, S. B., & Rattakorn, P. (2011). Unsupervised feature selection using weighted principal components. *Expert systems with applications, 38*, 5704-5710.

Klema, J., Flek, O., Kout, J., & Novakova, L. (2005). Intelligent Diagnosis and Learning in Centrifugal Pumps. In *Emerging Solutions for Future Manufacturing Systems* (pp. 513-522): Springer.

Lee, S., Jung, K.-H., Kim, J.-H., & Kang, S.-H. (2002). Cavitation mode analysis of pump inducer. *KSME International Journal, 16*, 1497-1510.

McKee, K., Forbes, G., Mazhar, I., Entwistle, R., & Howard, I. (2011). A review of machinery diagnostics & prognostics implemented on a centrifugal pump. In J. N. Jay Lee, Jag Sarangapani, Joseph Mathew (Ed.), *Proceedings of the 6th World Congress on Engineering Asset Management*. Cincinnati, OH, USA: Springer.

McKee, K. K., Forbes, G., Mazhar, I., Entwistle, R., & Howard, I. (2011). A review of major centrifugal pump failure modes with application to the water supply and sewerage industries. In *ICOMS Asset Management Conference* (pp. 32). Gold Coast, QLD.

McKee, K. K., Forbes, G. L., Mazhar, I., Entwistle, R., Howard, I., & Mapeza, T. (2012). Modification of the ISO-10816 centrifugal pump vibration severity charts for use with Octave band spectral measurements. In *Proceedings: the 7th Australasian Congress on Applied Mechanics (ACAM 7), 9 - 12 December 2012* (pp. 276-283). the University of Adelaide, North Terrace Campus / National Committee on Applied Mechanics of Engineers Australia. : Engineers Australia.

McKee, K. K., Forbes, G., Mazhar, I., Entwistle, R. and Howard, I. (2012). Modification of the ISO-10816 centrifugal pump vibration severity charts for use with Octave band spectral measurements. In *7th Australasian Congress on Applied Mechanics* (pp. 276- 283). Adelaide, SA: Engineers Australia.

McKee, K. K., Forbes, G., Mazhar, I., Entwistle, R., Hodkiewicz, M. and Howard, I. (2012). A Single Cavitation Indicator Based on Statistical Parameters For A Centrifugal Pump. In *World Congress on Engineering Asset Management*. Daejon, South Korea.

Neil, G. D., Reuben, R. L., Sandford, P. M., Brown, E. R., & Steel, J. A. (1997). Detection of incipient cavitation in pump using acoustic emission. *Proceedings of the Institution of Mechanical Engineers, 211*, 267 - 277.

Palgrave, R. (1989). Diagnosing Pump Problems From Their Noise Emissions Signature. In *New Challenges – Where Next? – 11th International Conference of the British Pump Manufacturers' Association* (pp. 9 - 28). UK: BHRA.

Parrondo, J. L., Velarde, S., & Santolaria, C. (1998). Development of a predictive maintenance system for a centrifugal pump. *Journal of Quality in Maintenance Engineering, 4*, 198 - 211.

Rapposelli, E., Cervone, Angelo, d'Agostino, Luca. (2002). A New Cavitating Pump Rotordynamic Test Facility. In *38th AIAA/ASME/SAE/ASEE Joint Propulsion Conference & Exhibit*. Indianapolis, Indiana: American Institute of Aeronautics and Astronautics, Inc.

Rayner, R. (1995). *Pump Users Handbook*. Oxford: Elsevier Advanced Technology

Rencher, A. C., & Christensen, W. F. (2012). Principal Component Analysis. In *Methods of Multivariate Analysis* (pp. 405-433): John Wiley & Sons, Inc.

Sakthivel, N. R., Sugumaran, V., & Babudevasenapati, S. (2010). Vibration based fault diagnosis of monoblock centrifugal pump using decision tree. *Expert systems with applications, 37*, 4040-4049.

Sakthivel, N. R., Sugumaran, V., & Nair, B. B. (2010). Comparison of decision tree-fuzzy and rough set-fuzzy methods for fault categorization of mono-block centrifugal pump. *Mechanical Systems and Signal Processing, 24*, 1887-1906.

Sloteman, D. P. (2007). Cavitation In High Energy Pumps - Detection And Assessment Of Damage Potential. In *23rd International Pump User Symposium* (pp. 29 - 38). George R. Brown Convention Center, Houston, TX, USA.

Standardization, I. O. f. (1975). ISO 532: Method for calculating loudness level. In. Switzerland: International Organization for Standardization.

Standardization, I. O. f. (1998). ISO 10816 - 3: Mechanical vibration - Evaluation of machine vibration by measurements on non-rotating parts - In *Part 3: Industrial machines with*

nominal power above 15 kW and nominal speeds between 120 r/min and 15 000 r/min when measured in situ. Switzerland: ISO.

Standardization, I. O. f. (2009). ISO 10816 - 7: Mechanical vibration - Evaluation of meachine vibration by measurements on non-rotating parts. In *Part 7: Rotodynamic pumps for industrial applications, including measurements on rotating shafts*. Switzerland: ISO.

Sunwater. (2012). Personal Communications with Staff at Sunwater. In. Bundaberg.

Toyota, T., Niho, T., & Peng, C. (2000). Condition Monitoring And Diagnosis Of Rotating Machinery by Gram-Charlier Expansion of Vibration Signal. In *Fourth International Conference on Knowledge-Based Intelligent Engineering Systems and Allied Technologies* (Vol. 2, pp. 541-544).

Uchiyama, T. (1998). Numerical simulation of cavitating flow using the upstream finite element method. *Applied Mathematical Modelling, 22*, 235-250.

Wang, H. (2010). Intelligent diagnosis methods for plant machinery. *Frontiers of Mechanical Engineering in China, 5*, 118-124.

Wang, H., & Chen, P. (2007). Sequential Condition Diagnosis for Centrifugal Pump SystemUsing Fuzzy Neural Network. *Neural Information Processing – Letters and Reviews 11*, 41-50.

Wang, H., & Chen, P. (2009). Intelligent diagnosis method for a centrifugal pump using features of vibration signals. *Neural Computing and Applications, 18*, 397-405.

Wang, P.-C., Su, C.-T., Chen, K.-H., & Chen, N.-H. (2011). The application of rough set and Mahalanobis distance to enhance the quality of OSA diagnosis. *Expert systems with applications, 38*, 7828-7836.

Wang, Y., Liu Hou, L., Yuan Shou, Q., Tan Ming, G., & Wang, K. (2009). Prediction research on cavitation performance for centrifugal pumps. In *Intelligent Computing and Intelligent Systems, 2009. ICIS 2009. IEEE International Conference on* (Vol. 1, pp. 137-140).

Wold, S., Esbensen, K., & Geladi, P. (1987). Principal component analysis. *Chemometrics and Intelligent Laboratory Systems, 2*, 37-52.

Yang, B.-S., Lim, D.-S., & Tan, A. C. C. (2005). VIBEX: an expert system for vibration fault diagnosis of rotating machinery using decision tree and decision table. *Expert systems with applications, 28*, 735-742.

Yedidiah, S. (1996). *Centrifugal pump user's guidebook : problems and solutions* New York: Chapman & Hall.

Zhang, Y., Huang, D., Ji, M., & Xie, F. (2011). Image segmentation using PSO and PCM with Mahalanobis distance. *Expert systems with applications, 38*, 9036-9040.

Zouari, R., Sieg-Zieba, S., & Sidahmed, M. (2004). Fault Detection System For Centrifugal Pumps Using Neural Networks and Neuro-Fuzzy Techniques. In *Surveillance 5 CETIM Senlis 11-13 October 2004*.